

${}^4\text{He}(\vec{p},d){}^3\text{He}$ reaction at 200 and 400 MeV

P. W. F. Alons, J. J. Kraushaar, and J. R. Shepard

Nuclear Physics Laboratory, Department of Physics, University of Colorado, Boulder, Colorado 80309

J. M. Cameron, D. A. Hutcheon, R. P. Liljestrand,* W. J. McDonald, C. A. Miller, and W. C. Olsen

Department of Physics, University of Alberta, Edmonton, Alberta, Canada T6G 2N5

J. R. Tinsley†

Department of Physics, University of Oregon, Eugene, Oregon 97403

C. E. Stronach

Department of Physics, Virginia State University, Petersburg, Virginia 23803

(Received 11 September 1985)

We have measured cross sections and analyzing powers for the ${}^4\text{He}(\vec{p},d){}^3\text{He}(\text{g.s.})$ reaction at 200 and 400 MeV. In contrast with the cross sections, angular distributions of the analyzing powers are highly structured. Exact finite range distorted-wave Born approximation calculations are compared with the data. Agreement with the present data is reasonable, but earlier 770 MeV cross section data are poorly described by this method.

I. INTRODUCTION

The ${}^4\text{He}(p,d){}^3\text{He}$ reaction possesses some appealing theoretical features. The nuclear structure involved is relatively simple since essentially only $1S$ orbitals can participate. Furthermore, the wave functions can be constrained by the wealth of experimental information on ${}^3\text{He}$ and ${}^4\text{He}$. This permits investigations of the reaction mechanism with a minimum of additional theoretical uncertainties. In particular, one may be able to learn about the role of pion emission and absorption processes as well as intermediate Δ formation in the (p,d) process. For such light systems exchange processes, in this case the two-nucleon pickup process ${}^4\text{He}(p,{}^3\text{He}){}^2\text{H}$, may also be important. In addition, knowledge of the cross sections over a wide energy range is useful in astrophysical calculations of the production of ${}^3\text{He}$. While there have been several studies at proton energies less than 100 MeV, there are very few published data at higher energies where there is a large momentum transfer. In addition, analyzing power measurements, which are most important in trying to assess the validity of the reaction mechanism being used, have only been taken at 32 and 50 MeV, although some unpublished data exist at 650 and 800 MeV.¹ In order to provide additional intermediate energy data on this reaction, the present measurements have been made at TRIUMF using the 1.4 GeV/ c spectrometer and beams of polarized protons of 200 and 400 MeV.

Although the details of the reaction mechanism appropriate for the (p,d) reaction on a very light target at an energy of several hundred MeV are not entirely clear, the data to be presented will be compared to exact-finite-range distorted wave calculations using the adiabatic approximation for the deuteron potential. These calculations will at least serve as a reference frame for discussing additional aspects of the reaction mechanism that should be in-

cluded in the calculations. In order to provide a consistent set of energy dependent optical potential parameters for the proton channel, proton- ${}^4\text{He}$ elastic scattering data from 85 to 800 MeV were fitted using a search procedure. Distorted-wave calculations were carried out and comparisons were made with existing data at 156 MeV (Ref. 2) and 770 MeV (Ref. 3) as well as with the data presented in this paper.

II. EXPERIMENTAL PROCEDURES

A polarized proton beam from the TRIUMF cyclotron was used in conjunction with the 1.4 GeV/ c magnet spectrometer (MRS) and a liquid ${}^4\text{He}$ target to carry out the measurements. Details of the apparatus and the method used in determining the polarization of the beam⁴⁻⁶ and the construction of the liquid ${}^4\text{He}$ target^{7,8} have been published previously. The polarization of the beam was typically 60% to 70% and was monitored continuously during a run by a polarimeter and a thin CH_2 foil that was inserted in the beam. The beam polarization was known to ± 0.03 . The liquid ${}^4\text{He}$ was about 33 mg/cm² thick and was contained in a cell that had separate kapton and nickel windows that were 0.15 mg/cm² thick.

The essential features of the magnetic spectrometer that are relevant to the present experiment have also been described previously.⁹ The momentum acceptance of the spectrometer was set at about $\pm 7\%$. Deuteron spectra at 200 and 400 MeV taken during the measurements have been published¹⁰ and the deuteron group to the ground state of ${}^3\text{He}$ is well resolved from the continuum with little background contribution.

Normalization of the cross sections was based on elastic ${}^4\text{He}(p,p)$ data, which were taken at 200 MeV at scattering angles of 16°, 30°, and 45° and compared to the published cross sections of Moss *et al.*¹¹ It is estimated that the un-

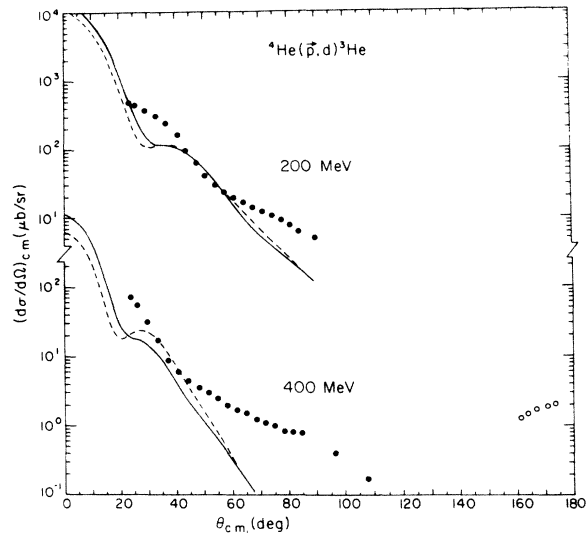


FIG. 1. Angular distributions for the ${}^4\text{He}(\bar{p},d){}^3\text{He}$ reaction taken with proton energies of 200 and 400 MeV. The solid lines are the results of exact-finite-range distorted wave calculations using a Gaussian-shaped form factor for the bound state calculations and for the dashed line a form factor derived from electron scattering on ${}^4\text{He}$ was used. The open circles at 400 MeV are from Ref. 12.

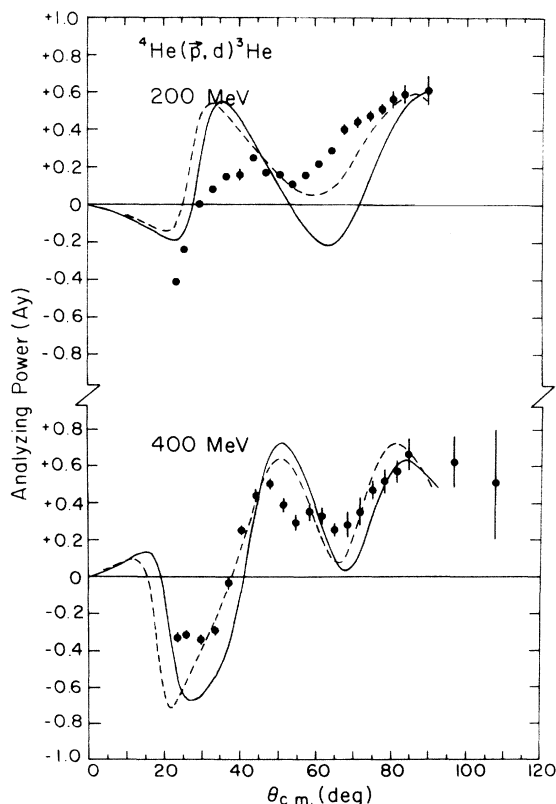


FIG. 2. Analyzing power data for the ${}^4\text{He}(\bar{p},d){}^3\text{He}$ reaction at 200 and 400 MeV. The solid and dashed lines are the results of calculations described in Fig. 1.

certainty in the absolute values of the cross sections is no larger than 20%.

The cross sections at 200 and 400 MeV are displayed in Fig. 1 and the analyzing power data in Fig. 2; the numerical values are shown in Table I. The error bars shown on these data are based on statistics only. Also shown in Fig. 1 as the open circles are the back angle cross section measurements of Cameron *et al.*¹² at 400 MeV.

III. DISTORTED WAVE CALCULATIONS

In order to provide optical model parameters for the incident protons in the DWBA calculations, a series of parameter searches were carried out with proton elastic scattering data on ${}^4\text{He}$ that ranged in energy from 85 to 800 MeV. Explicitly, elastic cross section and analyzing power data at 85 MeV,¹³ 200, 350, and 500 MeV,¹¹ and 800 MeV (Ref. 14) were used with the search program MAGALI,¹⁵ which was extended to include relativistic kinematics. In the search procedure the values of r_R and a_R , the radius and diffuseness parameter of the real potential, were fixed at 1.244 and 0.206 fm, and a_I , the diffuseness parameter for the imaginary volume potential, was fixed at 0.336 fm. With these restraints optimum values for V_R , W_I , r_I , V_{so} , r_{so} , and a_{so} were obtained for the elastic data at the five energies. In this way curves could be constructed for these parameters that varied smoothly in energy. The proton parameters at the four energies of interest for the (p,d) reaction were then taken from these plots and their values are shown in Table II.

The deuteron optical potentials used were based on the adiabatic deuteron approximation of Johnson and Soper.¹⁶ This was done in part because very few deuteron- ${}^3\text{He}$ elastic scattering data are available in the energy range of interest, but mainly because the adiabatic model compensates for the deuteron breakup effects. The actual deuteron parameters that were used are shown in Table II and were constructed from the $p + {}^4\text{He}$ potential parameters at one-half the corresponding deuteron laboratory energy generally following the prescription of Harvey and Johnson,¹⁷ while taking into account that the deuteron scatters from ${}^3\text{He}$ rather than ${}^4\text{He}$.

For the bound state of the transferred nucleon two form factors were used. The first form factor was a simple Gaussian 1S wave function from a harmonic oscillator well with a harmonic oscillator parameter, $b=1.42$ fm.¹⁸ This oscillator parameter was obtained by fitting the momentum distribution of protons measured in the ${}^4\text{He}(e,e'p)$ reaction¹⁹ with a Gaussian function.

The second form factor was derived using a procedure derived by Shepard *et al.*²⁰ Here the charge form factor obtained from electron- ${}^4\text{He}$ elastic scattering data was modified by subtracting pion exchange current contributions to give a true nucleon density. A Fourier transform was then taken of the modified charge density to yield a form factor whose numerical values were directly used in DWUCK5.²¹ This exact-finite-range program allows for the inclusion of nonlocal effects by the introduction of a nonlocality parameter, β . The values that were used at all energies were 0.85 for the incoming proton and 0.54 for the outgoing deuteron. Calculations were also carried out

TABLE I. Cross sections and analyzing power data for the ${}^4\text{He}(\bar{p},d){}^3\text{He}$ reaction at 200 and 400 MeV.

$\theta_{\text{c.m.}}$ (deg)	$d\sigma/d\Omega$ ($\mu\text{b}/\text{sr}$) _{c.m.}	A_y
$E_p=200$ MeV		
23.4	495 \pm 6	-0.41 \pm 0.02
25.6	462 \pm 6	-0.25 \pm 0.02
29.3	389 \pm 5	0.01 \pm 0.02
32.9	312 \pm 3	0.08 \pm 0.02
36.5	246 \pm 3	0.15 \pm 0.02
40.1	167 \pm 3	0.16 \pm 0.03
43.6	97.7 \pm 0.8	0.25 \pm 0.01
47.1	64.7 \pm 0.7	0.17 \pm 0.01
50.6	42.3 \pm 0.4	0.16 \pm 0.01
54.1	30.9 \pm 0.3	0.11 \pm 0.02
57.6	23.9 \pm 0.2	0.15 \pm 0.01
61.0	20.4 \pm 0.2	0.22 \pm 0.02
64.3	17.4 \pm 0.2	0.29 \pm 0.02
67.7	14.4 \pm 0.2	0.40 \pm 0.02
71.0	12.5 \pm 0.2	0.44 \pm 0.02
74.2	11.0 \pm 0.2	0.48 \pm 0.03
77.5	9.4 \pm 0.2	0.51 \pm 0.03
80.6	7.9 \pm 0.2	0.56 \pm 0.04
83.8	6.4 \pm 0.3	0.59 \pm 0.05
89.9	5.1 \pm 0.2	0.61 \pm 0.07
$E_p=400$ MeV		
23.7	72 \pm 1	-0.32 \pm 0.02
26.0	56.3 \pm 0.9	-0.31 \pm 0.02
29.7	31.5 \pm 0.8	-0.34 \pm 0.02
33.4	17.2 \pm 0.3	-0.29 \pm 0.02
37.0	8.7 \pm 0.2	-0.03 \pm 0.03
40.6	6.1 \pm 0.1	0.25 \pm 0.03
44.2	4.5 \pm 0.1	0.44 \pm 0.04
47.8	3.59 \pm 0.07	0.51 \pm 0.03
51.3	3.05 \pm 0.08	0.39 \pm 0.04
54.8	2.47 \pm 0.07	0.29 \pm 0.04
58.2	2.04 \pm 0.07	0.35 \pm 0.05
61.7	1.67 \pm 0.06	0.33 \pm 0.05
65.1	1.55 \pm 0.04	0.25 \pm 0.03
68.4	1.26 \pm 0.06	0.28 \pm 0.07
71.7	1.11 \pm 0.06	0.35 \pm 0.08
75.0	0.99 \pm 0.03	0.47 \pm 0.05
78.2	0.85 \pm 0.04	0.52 \pm 0.06
81.4	0.82 \pm 0.03	0.57 \pm 0.06
84.5	0.78 \pm 0.05	0.66 \pm 0.09
96.6	0.42 \pm 0.04	0.62 \pm 0.14
107.7	0.17 \pm 0.03	0.51 \pm 0.30

for both form factors with the nonlocal parameter set equal to zero. In the calculations shown, a spectroscopic factor of 2 has been assumed and is included in the calculations.

IV. CONCLUSIONS

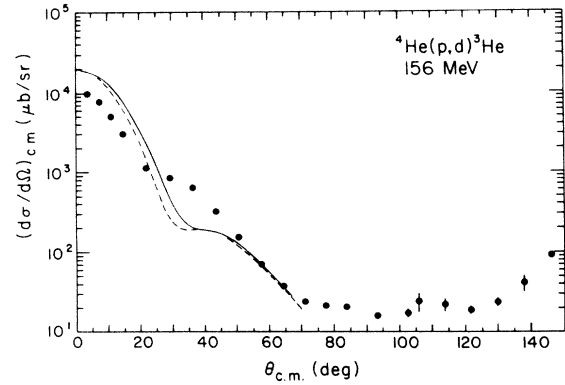
The comparison of the distorted wave calculations with the ${}^4\text{He}(p,d)$ cross section data is shown in Figs. 1, 3, and 4. At all four energies the theoretical description of the data is relatively poor. While the general magnitude of the cross sections is not in bad agreement, the detailed slopes of the theoretical angular distributions miss the shapes of the experimental data in a rather fundamental

way. The differences between the calculations carried out with the two different form factors for the bound state calculation are relatively minor except at 770 MeV, where the Gaussian form factor provides far less structure than does the one based on the charge density distribution of ${}^4\text{He}$.

As shown in Fig. 2, the calculations provide a reasonable description of the analyzing power data. At 400 MeV the description is most encouraging. The results of the calculations with the nonlocal parameter, β , set equal to zero are not shown in the figures. The effect on the cross sections of having $\beta=0$ was negligible. The effect on the analyzing power prediction at 156 and 200 MeV

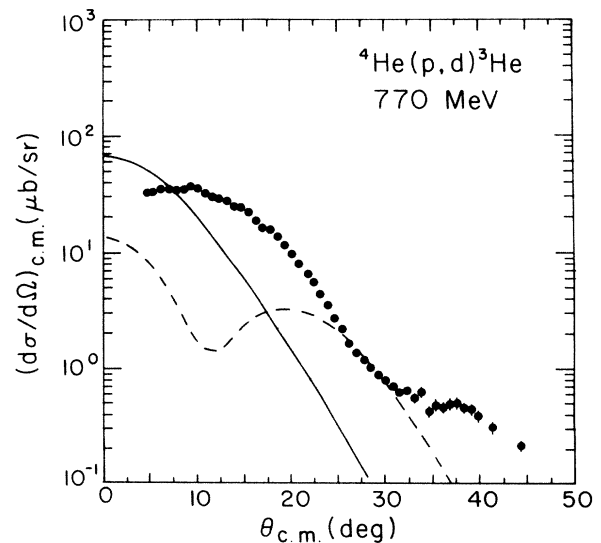
TABLE II. Optical model parameters.

T_p (MeV)	Channel	V_R (MeV)	r_R (fm)	a_R (fm)	W_I (MeV)	r_I (fm)	a_I (fm)	V_{so} (MeV)	r_{so} (fm)	a_{so} (fm)
156	p	-7.40	1.244	0.206	-13.45	1.494	0.336	-6.30	0.852	0.217
	d	-20.25	1.144	0.246	-18.09	1.72	0.40	-4.80	0.855	0.246
200	p	-3.64	1.244	0.206	-13.16	1.387	0.336	-5.75	0.857	0.228
	d	-16.650	1.164	0.246	-17.63	1.62	0.40	-4.54	0.853	0.249
400	p	+11.60	1.244	0.206	-9.50	1.480	0.336	-4.56	0.940	0.303
	d	+1.650	1.244	0.246	-16.88	1.37	0.40	-3.60	0.860	0.307
770	p	+20.00	1.244	0.206	-10.20	1.278	0.336	-1.80	0.969	0.266
	d	+22.875	1.244	0.246	-7.965	1.45	0.40	-2.37	0.980	0.336

FIG. 3. Angular distribution for the ${}^4\text{He}(p,d){}^3\text{He}$ reaction at 156 MeV (Ref. 2). The solid and dashed lines are the results of calculations as described in Fig. 1.

was to reduce rather drastically the magnitudes of A_p . At 400 and 770 MeV the effect was to change completely the angular dependence such as to destroy any agreement with the 400 MeV data.

It is clear that the pickup reaction mechanism that has been assumed is in general not accounting for the data in an adequate fashion. Apart from the direct one-nucleon transfer process, there are additional processes that may contribute to the ${}^4\text{He}(p,d)$ cross sections. Some of these are presented by the diagrams in Fig. 5. Figure 5(a) pictures the direct one-nucleon transfer assumed in the DWBA calculations presented. Figure 5(b) represents the "heavy particle stripping" contributions, which involve here a direct two-nucleon transfer. This coherent contribution is certainly expected to be more important here than for the case of a (p,d) reaction on heavier nuclei, where the heavy particle stripping involves the transfer of a (much) larger nuclear cluster. Calculations that include

FIG. 4. Angular distribution for the ${}^4\text{He}(p,d){}^3\text{He}$ reaction at 770 MeV (Ref. 3). The solid and dashed lines are the results of calculations as described in Fig. 1.

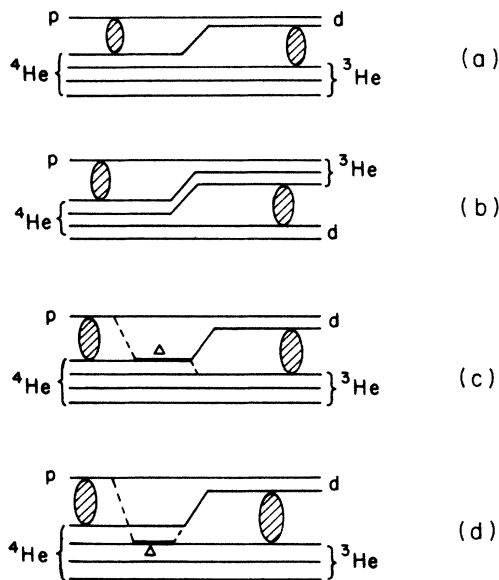


FIG. 5. Diagrams illustrating various possible contributions to the ${}^4\text{He}(p,d){}^3\text{He}$ cross section. The one- and two-nucleon transfer are shown in (a) and (b), respectively. The process of interaction through a delta is shown in (c) and (d) either directly with the transferred neutron or with a spectator.

this exchange contribution are being pursued. The rise in the cross sections at scattering angles greater than about 100° is clearly seen in the 156 MeV data and in the 400 MeV data between 160° and 180° . This is no doubt mainly due to the two-nucleon transfer. In fact, plane wave calculations carried out by Bernas *et al.*² account for this general back angle rise in the cross sections in terms of

this process. In a similar fashion, two-nucleon transfer calculations were carried out to account for the large angle (p,d) data taken at a proton energy of 85 MeV. It will be important to see the results for even the forward angle region when the one- and two-nucleon transfer contributions are added coherently.

Figures 5(c) and (d) represent processes in which the momentum transfer is shared between two nucleons, one nucleon becoming a delta. These processes may be expected to give substantial contributions at higher energies, because of the momentum mismatch which is especially important for $l=0$ transitions. Calculations of the general type indicated in diagram 5(c) were carried out by Boudard *et al.*²² for the ${}^{16}\text{O}(d,p){}^{17}\text{O}$ reaction at $E_d=698$ MeV. Here the one-nucleon stripping cross sections alone overpredicted the measured cross sections by a factor of about 7. Inclusion of double pion rescattering with intermediate Δ excitation had the general effect of reducing the predicted cross sections to achieve reasonable agreement with the data but the shape was poorly reproduced. In a subsequent publication, however, Shepard and Rost²³ were able to account reasonably well for these same data with an exact-finite-range single neutron transfer distorted wave calculation.

ACKNOWLEDGMENTS

The authors wish to express their appreciation to H. S. Wilson and G. Hassold for their help in conducting the experiment. This work was supported in part by the U.S. Department of Energy, the Natural Sciences and Engineering Research Council of Canada, and the U.S. National Aeronautics and Space Administration.

*Present address: E.G. and G. Energy Measurements, Inc., Los Alamos, NM 87545.

†Present address: Laboratoire National Saturne, CEN Saclay, 91191 Gif-sur-Yvette, Cedex, France.

¹J. R. Shepard, R. L. Boudrie, N. S. P. King, G. Igo, A. Rahbar, B. Aas, C. A. Witten, M. Gazzally, and G. S. Adams (unpublished).

²M. Bernas, D. Bachelier, J. K. Lee, R. Radvanyi, M. Roy-Stéphan, I. Brissaud, and C. Detraz, Nucl. Phys. A156, 289 (1970).

³T. Bauer, A. Boudard, H. Catz, A. Chaumeaux, P. Couvert, M. Gardon, J. Guyot, D. Legrand, J. C. Lugol, M. Matoba, B. Mayer, J. P. Tabet, and Y. Terrien, Phys. Lett. 67B, 265 (1977).

⁴A. W. Stetz, J. M. Cameron, D. A. Hutcheon, R. H. McCamis, C. A. Miller, G. A. Moss, G. Roy, J. G. Rogers, C. A. Goulding, and W. T. H. van Oers, Nucl. Phys. A290, 285 (1975).

⁵R. H. McCamis, J. M. Cameron, L. G. Greeniaus, D. A. Hutcheon, C. A. Miller, G. A. Moss, G. Roy, M. S. de Jong, B. T. Murdoch, W. T. H. van Oers, J. G. Rogers, and A. W. Stetz, Nucl. Phys. A302, 388 (1978).

⁶L. G. Greeniaus, D. A. Hutcheon, C. A. Miller, G. A. Moss, G. Roy, R. Dubois, C. Amsler, B. K. S. Koene, and B. T. Murdoch, Nucl. Phys. A322, 308 (1979).

⁷C. A. Goulding, B. T. Murdoch, M. S. de Jong, W. T. H. van

Oers, and R. H. McCamis, Nucl. Instrum. Methods 148, 11 (1978).

⁸R. H. McCamis, Ph.D. thesis, University of Alberta, 1977 (unpublished).

⁹G. A. Moss, C. A. Davis, J. M. Greben, L. G. Greeniaus, G. Roy, J. Uegaki, R. Abegg, D. A. Hutcheon, C. A. Miller, and W. T. H. van Oers, Nucl. Phys. A392, 361 (1983).

¹⁰J. Källne, J. Phys. G 8, 1371 (1982).

¹¹G. A. Moss, L. G. Greeniaus, J. M. Cameron, D. A. Hutcheon, R. L. Liljestrang, C. A. Miller, G. Roy, B. K. S. Koene, W. T. H. van Oers, A. W. Stetz, A. Willis, and N. Willis, Phys. Rev. C 21, 1932 (1980).

¹²J. M. Cameron, L. G. Greeniaus, D. A. Hutcheon, R. H. McCamis, C. A. Miller, G. A. Moss, G. Roy, M. S. de Jong, B. T. Murdoch, W. T. H. van Oers, J. G. Rogers, and A. W. Stetz, Phys. Lett. 74B, 31 (1978).

¹³L. G. Votta, P. G. Roos, N. S. Chant, and R. Woody III, Phys. Rev. C 10, 520 (1974).

¹⁴H. Courant, K. Einsweiler, T. Joyce, H. Kagan, Y. I. Makdisi, M. L. Marshak, B. Mossberg, E. A. Peterson, K. Ruddick, T. Walsh, G. J. Igo, R. Talaga, A. Wriekat, and R. Klem, Phys. Rev. C 19, 104 (1979).

¹⁵Program MAGALI, J. Raynal, private communication.

¹⁶R. C. Johnson and P. J. R. Soper, Phys. Rev. C 1, 976 (1970).

¹⁷J. D. Harvey and R. C. Johnson, Phys. Rev. C 3, 636 (1971).

- ¹⁸P. J. Brussard and P. W. M. Glaudemans, *Shell Model Applications in Nuclear Spectroscopy* (North-Holland, Amsterdam, 1977), p. 3.
- ¹⁹V. A. Goldstein, Eh. L. Kuplennikov, R. I. Jubuti, and R. Ya. Kezerashvili, *Nucl. Phys.* **A355**, 333 (1981).
- ²⁰J. R. Shepard, E. Rost, and G. R. Smith, *Phys. Lett.* **89B**, 13 (1979).
- ²¹P. D. Kunz, computer program, University of Colorado (unpublished).
- ²²A. Boudard, Y. Terrien, R. Beurtey, L. Bimbot, G. Bruge, A. Chaumeaux, P. Couvert, J. M. Fontaine, M. Gargon, Y. LeBornec, D. Legrand, L. Schecter, J. P. Tabet, and M. Dillig, *Phys. Rev. Lett.* **46**, 218 (1981).
- ²³J. R. Shepard and E. Rost, *Phys. Rev. Lett.* **46**, 1544 (1981).